IOSR Journal of Mechanical and Civil Engineering (IOSR-JMCE)
e-ISSN: 2278-1684,p-ISSN: 2320-334X, Volume 15, Issue 6 Ver. I (Nov. - Dec. 2018), PP 58-65
www.iosrjournals.org

To investigate effect of mesh number and different turbulent models on numerical simulation of a container ship's propeller.

Vu Van Duy[1], Truong Viet Anh[2] , Pham Ngoc Anh[1], Nguyen Chi Cong [1,2*]
[1]*Vietnam Marine University, 180000, Haiphong, Vietnam*
[2]*Hanoi University of Science and Technology, 10000, Hanoi, Vietnam*
Corresponding Author: Nguyen Chi Cong

Abstract: *The main objective of the paper is to investigate the effect of mesh number and different turbulent models on numerical simulation of a marine propeller. The analyzed propeller is at the following design condition: The diameter of 3,65 m; speed of 200 rpm; average pitch of 2,459 m, boss ratio of 0,1730. The first stage involves the mesh generation and refinement on domain of the designed propeller. The second stage deals with the identification of initial and boundary conditions of the mesh-equipped module. In the final stage, the authors give the hydrodynamic performance of the propeller and various results are calculated to examine effect of those factors on simulation results.*

Keywords: *CFD, propeller, mesh number.*

Date of Submission: 10-11-2018 Date of acceptance: 25-11-2018

I. Introduction

At present with the development of computer science, the computational fluid dynamics (CFD) play important role in simulating and calculating flow fields around different geometries using numerical methods and established algorithms. During recent years, considerable progress in the field of computer science has donated to the decrease of computational costs of CFD simulations, making it more accessible for practical applications. Nowadays, the role of CFD methods is increasing in most fluid dynamics applications including the process of a ship's propeller design.

Simulating the aforementioned experiments provides the opportunity to obtain desired results by analyzing calculated flow characteristics. It can be a practical way of obtaining valid results at relatively low costs and in reasonable time compared with the real experiments. Since the self-propulsion test simulation is still quite expensive and time demanding, the common practice is to simulate only the open water test and to use its results to determine of self-propulsion characteristics. It can be done by taking into account established interaction factors accounting for the interaction between the hull resistance and open water characteristics of the propeller. In 2003, Takayuki WATANABE, Takafumi KAWAMURA, Yoshihisa TAKEKOSHI, Masatsugu MAEDA, Shin Hyung RHEE in the university of Tokyo used the Ansys Fluent software to study steady and unsteady cavitation on a marine propeller [1]. In 2008, at the RINA conference J. Bosschers, G. Vaz, A.R. Starke, E. van Wijngaarden in the Maritime Research Institute Netherlands utilized CFD to analyze of propeller sheet cavitation and propeller-ship interaction [2] . In 2012, Kinnas, Spyros A.Tian, Ye Sharma, Abhinav in the Ocean Engineering Group, Department of Civil, Architectural and Environmental Engineering, University of Texas at Austin employed the research of a Marine Propeller undergoing surge and heaveMotion by using CFD code [3]. In 2015, Lin Lu and his colleagues in the School of Marine Science and Technology, Northwestern Polytechnical University used CFD to predict and simulate a pumpjetpropulsor[4]. In 2017, Kurt Mizzi, Yigit Kemal Demirel, Charlotte Banks, Osman Turan, PanagiotisKaklis, Mehmet Atlar in the Department of Naval Architecture, Ocean and Marine Engineering, University of Strathclyde have employed CFD to design optimization of propeller boss cap fins for enhanced propeller performance[5].

In this work, three turbulent RNG k- ε, k-ϖ SST, and transition SST k-ϖ models with different mesh numbers were employed to predict the hydrodynamic performance of the Container Tan Cang Foundation ship's propeller. The simulation results, such as pressure distribution, velocity field and so on , are discussed, and the effect of the selected turbulent models and mesh number on the calculation result is also thoroughly examined.

II. Mathematical basis

2.1. Theoretical basis

The open water characteristics of a propeller are usually given in terms of the advance coefficient J, the thrust coefficient K_T, the torque coefficient K_Q and the open water efficiency η . Here, assuming constant rotational speed, the range of advance velocity (inlet velocity) values corresponding with advance coefficients of 0.1 to 0.75 is achieved. A complete computational solution for the flow was obtained using fluent software. The software estimated thrust and torque for different advance velocities. These were expressed in terms of K_T and K_Q which are defined as follows [6-10]:

Thrust coefficient:

$$K_T = \frac{T}{\rho n^2 D^4} \quad [1]$$

Torque coefficient :

$$K_Q = \frac{Q}{\rho n^2 D^5} \quad [2]$$

Advance coefficient

$$J = \frac{V_a}{nD} \quad [3]$$

Propellerefficiency

$$\eta_0 = \frac{K_T.J}{K_Q.2\pi} \quad [4]$$

2.2. Numerical simulation method

The governing equations for the turbulent incompressible flow encountered in this research are the three-dimensional RANS equations for the conservation of mass and momentum, given as [8,9,11,13]:

- **Conservation of mass**

$$\frac{\partial}{\partial x_i}\left(\rho \overline{u_i}\right) = 0 \quad [5]$$

- **Conservation of momentum**

$$\frac{\partial}{\partial t}\left(\rho \overline{u_i}\right) + \frac{\partial}{\partial x_j}\left(\rho \overline{u_i}\,\overline{u_j}\right) = \rho \overline{F_i} - \frac{\partial \overline{p}}{\partial x_j}\left[\mu\left(\frac{\partial \overline{u_i}}{\partial x_j} + \frac{\partial \overline{u_j}}{\partial x_i}\right)\right] \quad [6]$$

where $\overline{p}$ is the average pressure, μ is the molecular viscosity and $\rho \overline{u_i}\,\overline{u_j}$ is the Reynolds stress. To correctly account for turbulence, the Reynolds stresses are modeled in order to achieve the closure of Equation (2). An μ_t eddy viscosity is used to model the turbulent Reynolds stresses [6].

$$-\rho \overline{u_i' u_j'} = \mu_t\left(\frac{\partial \overline{u_i}}{\partial x_j} + \frac{\partial \overline{u_j}}{\partial x_i}\right) - \frac{2}{3}\delta_{ij}.\left(\rho k + \mu_t \frac{\partial \overline{u_i}}{\partial x_i}\right) \quad [7]$$

Where μ_t is the turbulent viscosity and k is the turbulent kinetic energy.

III. Computation and grid.

3.1. Geometry, computational domain, and mesh

In this study, the four-blade propeller of the Container Tan CangFouadation ship is selected for the numerical investigation. The detail parameters of the ship and its propeller are shown in the table 1 and table 2 below.

The first stage in simulation process is to build the geometry model for the problem. It plays important role in simulating and affecting directly in calculation results, so you should do your best when creating geometry. In this article, the team used the Solidworks software, with many advantage in designing complex surfaces and geometry, to create the geometry for all calculations. The next stage is to construct the calculation domain, suitable space surrounding the ducted propeller with appropriate sizes. In this work, the domain is a cylinder, with the length of thirteen times of the propeller's diameter and the diameter of seven times of the propeller's diameter, divided two components: the static domain and rotating domain. In the third step, the domain is imported, meshed, and refined in the Ansys meshing ICEM tool. All domains are meshed by using tetra mesh in which the rotating domain is modeled with smooth mesh, and the static domain takes the coarse, then converted into polyhedral mesh to save calculation time and improve accuracy for simulation results.

Table 1: Main parameters of the sip and its propeller

Main parameters of the ship

No	Name	Value	Unit
1	L.O.A	112.5	m
2	L.B.P	105.28	m
3	Breadth	18.2	m
4	Depth	6.7	m

Propeller detail parameter

	Parameters	**Value**	**Unit**
1	Diameter	3.650	m
2	Pitch	2.459	m
3	Revolution	200	rpm
4	Number of blade	4	
5	Rake	10	Deg
6	Screw	25	Deg
7	Blade thickness ratio	0.049	10
8	Cross section	Naca 66, a=0.8	

3.2. The number of mesh cases for investigating the propeller's performance

The quality of computational grid plays important role and directly affects the convergence and results of numerical analysis. To determine effects of mesh number on calculation results, the team employed calculations for eight different numbers of mesh in the same investigated domain. The mesh detail in the cases were shown in the table below.

Table 2: Mesh detail for different cases

Case 1

Domain	Nodes	Elements	Polyhedra
Dynamicfluid	1384067	279615	279615
Staticfluid	605933	112956	112956
All Domains	1990000	392571	392571

Case 2

Domain	Nodes	Elements	Polyhedra
Dynamicfluid	1495727	299751	299751
Staticfluid	605954	112956	112956
All Domains	2101681	412707	412707

Case 3

Domain	Nodes	Elements	Polyhedra
Dynamicfluid	1649594	326437	326437
Staticfluid	696020	128913	128913
All Domains	2345614	455350	455350

Case 4

Domain	Nodes	Elements	Polyhedra
Dynamicfluid	1995686	389680	389680
Staticfluid	696020	128913	128913
All Domains	2691706	518593	518593

Case 5

Domain	Nodes	Elements	Polyhedra
Dynamicfluid	1895640	371693	371693
Staticfluid	1054202	194548	194548
All Domains	2949842	566241	566241

Case 6

Domain	Nodes	Elements	Polyhedra
Dynamicfluid	1895524	371644	371644
Staticfluid	1791383	325457	325457
All Domains	3686907	697101	697101

Case 7

Domain	Nodes	Elements	Polyhedra
Dynamicfluid	1995686	389680	389680
Staticfluid	2061878	372818	372818
All Domains	4057564	762498	762498

Case 8

Domain	Nodes	Elements	Polyhedra
Dynamicfluid	1469699	292457	292457
Staticfluid	3026404	534419	534419
All Domains	496103	826876	826876

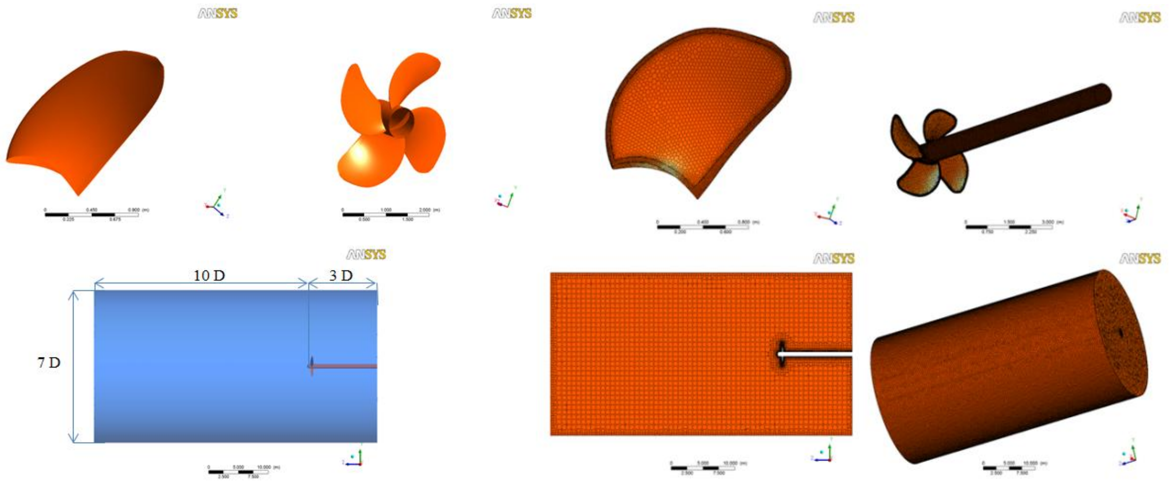

Figure 1: Geometry and mesh for computation

3.3. Boundary condition.

In this paper, the RNG k-ε, SST k- ω and the transition SST k - ω models are selected to investigate the effects of two factors on the propeller's hydrodynamic features; one is the effect's turbulence model on the calculation results; the other is the effect of the duct on the propeller's hydrodynamic characteristics. Velocity inlet is selected as inlet boundary condition. Assume that inlet velocity is uniform , axial and its value equals to the advance velocity of the ship . Pressure outlet is specified as the outlet boundary condition, and gauge pressure on the outlet is set to be 0 Pa. As to wall boundary condition, no slip condition is enforced on wall surface and standard wall function is also applied to adjacent region of the walls. Moving reference frame (MRF) is used to establish the moving coordinate system rotating with the propeller synchronously and the stationary coordinate system fixed on static shaft of the propeller, respectively . The first order upwind scheme with numerical under- relaxation is applied for the discretization of the convection term and the central difference scheme is employed for the diffusion term. The pressure - velocity coupling is solved through the PISO algorithm. Convergence precision of all residuals is under 0.0001. The details of boundary conditions are shown in table 4 [8,9,10,15,18].

Table 3: Boundary condition for simulation.

Name	Conditions	Value	Unit
Inlet	Velocity inlet	1.22-9.15	m/s
Outlet	Pressure inlet	0	pa
Wall	Static wall	-	-
Static domain	Static fluid	-	-
Dynamic domain	Rotating	200	rpm

IV. Resultand discussion

4.1. Effect of the mesh number on calculation results

The hydrodynamic coefficients of the studied propeller at the advance ratio J of 0.2 corresponding with eight cases was shown in the figure 2. From this, we can conclude that the mesh number plays an important role in calculating and simulating. In this paper, when the mesh number goes up from 300000 to 500000 elements, the hydrodynamic coefficients of the propeller also increases. However, when the mesh number reaches to the specific value in the range of 500000-800000 element, those factors, featured for the investigated propeller, remain the same. However, to facilitate further study, the number of mesh node in the six case was selected for the next analysis.

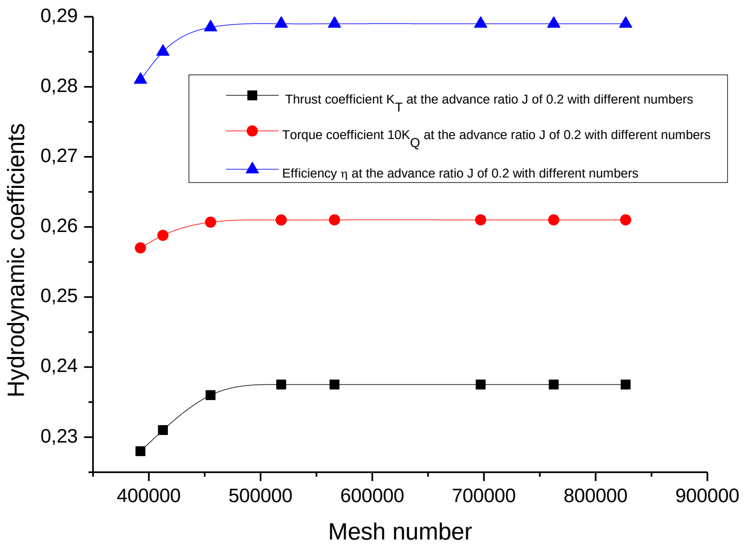

Figure 2: Hydrodynamic coefficients of the propeller with different mesh number at J of 0.2.

4.2. Hydrodynamic performance of the studied propeller

The figure 3 shows the pressure distribution on the back and pressure face of the studied propeller at the different advance ratios. The principle of distribution pressure on the two faces of the blade satisfies the theoretical law of the axial turbo- machinery. There is the pressure difference between the pressure face and the back face of the propeller in operation, and that difference makes the propeller thrust to overcome the ship hull resistance. The pressure distribution on the two faces of the blade depends on the advance ratio or velocity in let, the smaller advance ratio, the higher thrust. At the operating condition of the ship J = 0.6, on the pressure face, the almost area of the blade having the maximum pressure value is about $7.2.10^4$ Pa, the other at the blade leading towards the hub having the minimum pressure is about $-4.8.10^{-4}$ Pa, while the almost area of the suction face has the pressure in the range of $-1.2.10^{-5}$-$1.2.10^{-4}$ Pa . This means that the fluid accelerates as it approaches the propeller due to low pressure in the front of the propeller and the water continues to accelerate while it leaves the propeller.

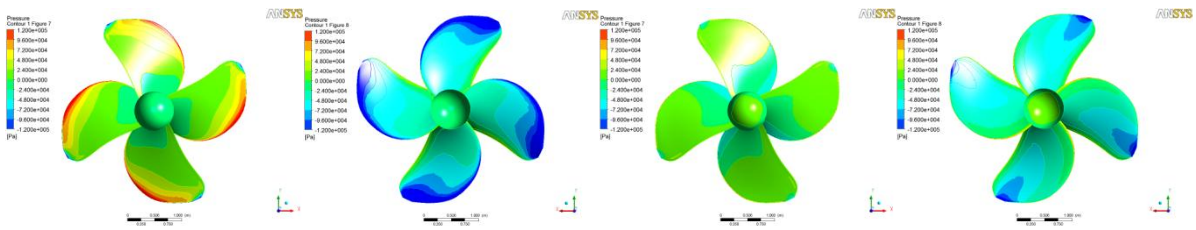

Figure 3: Pressure distribution on propeller faces at J =0.1 and 0.6 with n = 200rpm.

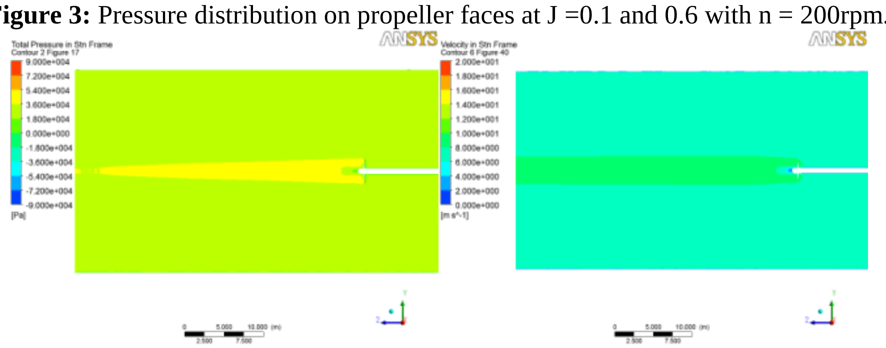

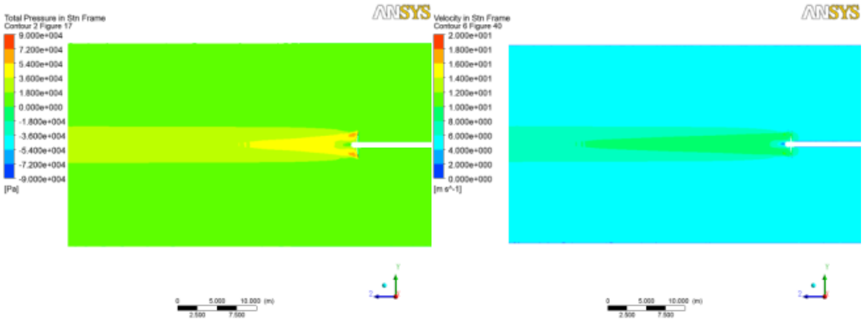

Figure 4: Total pressure and velocity distribution on axial plane at J = 0.5, 0.6.

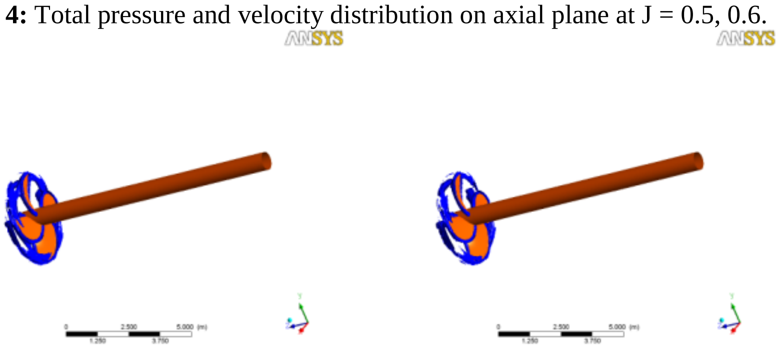

Figure 5: Vorticity surrounding the propeller at J = 0.2, 0.3.

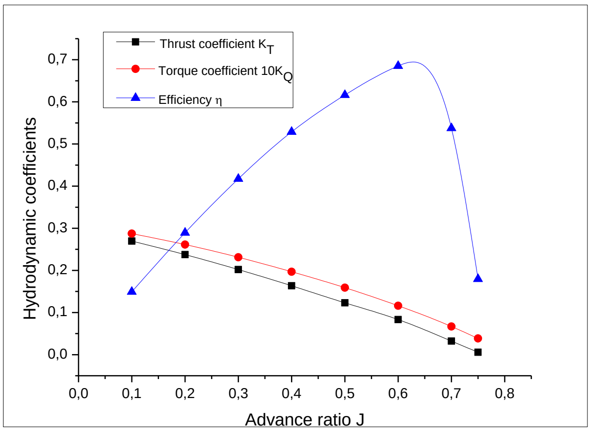

Figure 6: Propeller characteristic curves

The figure 4 shows the velocity and pressure distribution on the axial plane at the various advance ratio. As can be seen, due to pressure difference between two faces of propeller blade, the fluid toward the suction side is attracted because of the low pressure on this face to make the flow accelerate, and the fluid continues accelerating at the pressure face because of high pressure on it. When advance ratio J goes up, the pressure difference between them reduces. As a result, the difference of velocity before the suction side and after the pressure side also decrease. However the maximum velocity after the propeller in almost cases is about 12m/s, and the region towards the hub has the minimum velocity about -0.1m/s. This state having the contrary flow at the region.

The figure 6 presents the characteristic curves of the propeller is the function of advance ratio. Those are absolutely appropriate with the theory of wing and turbo- machinery stated in [5-18]. The changing principle of thrust and torque coefficient is linear with the advance ratio, and the maximum thrust and torque coefficients are 0,269, 0,01 respectively. The efficiency curve is slightly different in which it conforms to the linear principle with small advance ratio in range of 0.1 - 0.4, and the maximum efficiency is 0.66 with advance ratio 0.6 at the initially designed optimal point.

4.3. Effect of the turbulent models on calculation results

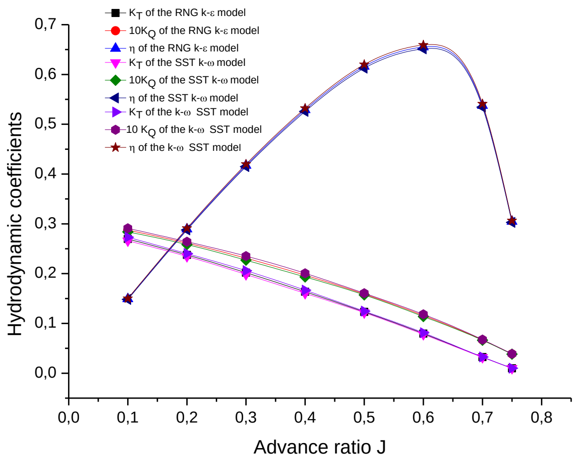

Figure 7: Hydrodynamic performance of the studied propeller with different turbulent models

The obtained results with three different turbulent models presented in the figure 7 reveals that the selected turbulent models have the slight impact on the calculation results. With the k - ω SST model, the propeller's efficiency gets the minimum value about 0.651 while the maximum efficiency of the studied propeller is about 0.659 with the transition SST k - ω model corresponding with the advance ratio J of 0.6. In the same way, thrust coefficient of the propeller gets the maximum about 0.273 with the transition SST k - ω model and the minimum about 0.266 with the k- ω SST model. With the propeller's torque coefficient, the maximum and minimum values are about 0.291, 0.284 respectively corresponding with the transition SST k - ω model and the k - ω SST model. However, the error of the investigated parameters among the selected models, being relatively small about 1.39 %, can be negligible in the calculation.

V. Conclusion.

In this paper, the propeller of the Container Tan Cang Foundation ship was analyzed at different advance ratios to construct the characteristic curves. There are some obtained results in the paper.

– This paper covers the process of CFD simulation of the open water test for a ship propeller and reveals its characteristic curves. When the advance ratio J goes up, the thrust and torque factor decrease constantly and reversely the efficiency of the propeller increases gradually with the advance ratio J in the range of 0.1-0.6. The maximum efficiency of the propeller got in this study about 0.66 at the advance ratio J of 0.6.
– The simulation for the investigated propeller was carried out with the eight cases of different mesh numbers. The obtained results reveals that in numerical simulation, the mesh number plays significantly important role so the first step in simulating a problem is to have to determine the appropriate mesh number in which the simulation results is constant. In this research, the authors employed calculating and simulating the propeller in the same domain with eight different mesh numbers, and realized that with the mesh number in the range of 500000-800000, the simulation results is the same.
– Three turbulence models were employed to investigate the effects of different turbulence models on the simulation results. The achieved outcomes suggest that the chosen turbulence models have the inconsiderable effect on the simulation results, and can ignore.

References.

[1]. Takayuki WATANABE, T.K., Yoshihisa TAKEKOSHI, Masatsugu MAEDA, Shin Hyung RHEE, Simulation of steady and unsteady cavitation on a marine propeller using a RANSCFD code. 2003: p. 8.
[2]. J. Bosschers, G.V., A.R. Starke, E. van Wijngaarden, Computational analysis of propeller sheet cavitation and propeller-ship interaction. RINA conference "MARINE CFD2008, 2008: p. 13.
[3]. Kinnas, S.A., Y. Tian, and A. Sharma, Numerical Modeling of a Marine Propeller Undergoing Surge and Heave Motion. International Journal of Rotating Machinery, 2012. 2012: p. 1-8.
[4]. Chen, Z., CFD Investigation in Scale Effects on Propellers with Different Blade Area Ratio. 2015: p. 71.
[5]. Kurt Mizzi∗, Y.K.D., Charlotte Banks, Osman Turan, and M.A. PanagiotisKaklis, Design optimisation of Propeller Boss Cap Fins for enhanced propeller performance. 2017.
[6]. ANSYS Fluent Theory Guide. 2013: p. 814.
[7]. Oosterveld, M.W.C.. Wake adapted ducted propellers. Tech. Rep. 345; Netherlands Ship Model Basin; 1970.
[8]. Horn, F.. Beitragzurtheorieummantelterschiffsschrauben. Jahrbuch der schiffbautechnischenGesellschaft 1940;:106-187.
[9]. Horn, F., Amtsberg, H.. Entwurf von schiffsdusensystemen (kortdusen). Jahrbuch der schiffbautechnischenGesellschaft 1950;44:141-206.

[10]. Ktichemann, D., Weber, J.. Aerodynamics of propulsion. McGraw-Hill; 1953.

[11]. Tachmindji, A.J.. The potential problem of the optimum propeller with finite number of blades operating in a cylindrical duct. Journal of Ship Research 1958;2(3):23-32.

[12]. Ordway, D.E., Sluyter, M.M., Sonnerup, B.O.U.. Three-dimensional theory of ducted propellers. 1960.

[13]. Morgan, W.B.. A theory of the ducted propeller with a finite number of blades. Tech. Rep.; University of California, Berkeley, Institute of engineering research; 1961.

[14]. Morgan, W.B.. Theory of the annular airfoil and ducted propeller. In: Proceedings of the Fourth Symposium on Naval Hydrodynamics. 1962, p. 151-197.

[15]. Dyne, G.. A method for the design of ducted propellers in a uniform flow. Tech. Rep. 62; SSPA; 1967.

[16]. Ryan, P.G., Glover, E.J.. A ducted propeller design method: a new approach using surface vorticity distribution techniques and lifting line theory. TransRINA 1972;114:545-563.

[17]. Morgan, W.B.,Caster, E.B.. Comparison of theory and experiment on ducted propellers. In: Cooper, R.D.,Doroff, S.W.,editors. Proceedings of the 7th Symposium on Naval Hydrodynamics. 1968, p. 1311-1349.

[18]. Caracostas, N.. Off design performance analysis of ducted propellers. In: Proceedings Propellers/Shafting '78 Symposium, SNAME. 1978, p. 3.1-3.8.

Nguyen Chi Cong. "To investigate effect of mesh number and different turbulent models on numerical simulation of a container ship's propeller.." IOSR Journal of Mechanical and Civil Engineering (IOSR-JMCE) , vol. 15, no. 6, 2018, pp. 58-65.